

Strange nonchaotic attractors of the damped pendulum with quasiperiodic forcing

Filipe J. Romeiras* and Edward Ott

Laboratory for Plasma and Fusion Energy Studies, University of Maryland, College Park, Maryland 20742

(Received 19 November 1986)

We discuss the existence and properties of strange nonchaotic attractors for the damped pendulum equation with two-frequency quasiperiodic forcing. In particular we present evidence that the equation does indeed exhibit strange nonchaotic attractors and that these attractors are *typical* [in the sense that they exist on a (Cantor) set of positive Lebesgue measure in parameter space]. We also show that the strange nonchaotic attractors have distinctive frequency power spectral characteristics which may make them observable in experiments involving physical nonlinear phenomena which can be modeled by the damped-forced-pendulum equation (e.g., Josephson junctions and sliding charge-density waves). Finally the transition to chaotic behavior is illustrated.

I. INTRODUCTION

Theoretical and experimental studies of periodically forced nonlinear systems have been of interest from a number of points of view. A prominent example of such a system is the equation

$$\frac{d^2\theta}{dt^2} + \nu \frac{d\theta}{dt} + \sin\theta = f(t), \quad (1)$$

where the forcing $f(t)$ is periodic in time, for example,

$$f(t) = K + V \cos(\omega t). \quad (2)$$

Equation (1) applies to a number of physical situations and, for this reason, it has received much attention. These situations include forced damped pendula, the Stewart-McCumber model of the current-driven Josephson junction¹ and a simple phenomenological model of sliding charge-density waves.² Past work on Eqs. (1) and (2) has demonstrated a wealth of characteristic nonlinear dynamical phenomena: strange attractors, period doubling cascades, mode locking, quasiperiodicity, crises, intermittency, fractal basin boundaries, etc. Indeed, Eqs. (1) and (2) are perhaps the most extensively investigated differential system for exhibiting low-dimensionality chaotic dynamics.

Equations (1) and (2) represent a periodically forced system. It is natural to ask what happens when the forcing $f(t)$ is quasiperiodic, rather than periodic; for example,

$$f(t) = K + V[\cos(\omega_1 t) + \cos(\omega_2 t)], \quad (3)$$

where ω_1 and ω_2 are incommensurate. That is, what new characteristic phenomena can be expected in quasiperiodically forced systems? This question is particularly apt, since, from the experimental point of view, using quasiperiodic rather than periodic forcing generally does not result in a major increase in the cost or complexity of an experiment. Indeed, some experiments using quasiperiodic forcing have already been done.^{3,4} In Ref. 3 the authors consider the transition from quasiperiodicity to chaos in an electronic Josephson-junction simulator driven by two

independent ac sources. In Ref. 4 the authors report that on experiments in an electron-hole plasma in germanium excited by two-frequency quasiperiodic external perturbations they observed stable three-frequency quasiperiodic states and transitions between three-frequency quasiperiodicity, two-frequency mode locking, and chaos.

Besides these two experimental works the above question has been addressed in Refs. 5–9. In Ref. 5 the authors consider the various routes to chaos in a quasiperiodically forced system governed by a two-dimensional map. In Ref. 6 the author discussed three-frequency quasiperiodic motion and its transition to two-frequency quasiperiodic motion and chaos in a quasiperiodically forced system described by a two-dimensional map (similar to that of Ref. 5). In Refs. 7–9, the authors examine the characteristics of *strange nonchaotic* attractors for quasiperiodically forced systems governed, respectively, by two-dimensional maps⁷ and first-order ordinary differential equations.^{8,9} This subject is also our main concern in this paper. Here the word *strange* refers to the geometrical structure of the attractor: A strange attractor is an attractor which is neither a finite set of points, a closed curve (like a limit cycle), a smooth (or piecewise smooth) surface (for example, a torus), or a volume bounded by a piecewise smooth closed surface. The word *chaotic* refers to the dynamics of orbits on the attractor: A chaotic attractor is one for which typical nearby orbits diverge exponentially with time (i.e., at least one Lyapunov exponent is positive). By a strange nonchaotic attractor we therefore mean an attractor which is geometrically strange, but for which typical orbits have nonpositive Lyapunov exponents. The two main results of Refs. 7–9 are the following.

(i) Strange nonchaotic attractors appear to be typical in quasiperiodically forced systems. That is, if we consider that the system is characterized by some parameter, then there is a set of positive measure in the parameter space for which strange nonchaotic attractors occur. To put it differently, if one picks a single parameter value at random, then the probability of this parameter value yielding a strange nonchaotic attractor is not zero. This typicality is unlike the situation occurring for other more familiar

dynamical systems, that are not quasiperiodically forced, for which strange nonchaotic attractors do occur, but they do so only on a set of zero measure in the parameters. (For example, the quadratic map $x_{n+1} = C - x_n^2$ exhibits a strange nonchaotic attractor precisely at the values of C where there is an accumulation of an infinite number of period doublings.) The fact that strange nonchaotic attractors are typical in quasiperiodically forced systems makes them easier to find and motivates further investigation to discover their observable properties [cf. point (ii), below].

(ii) The strange nonchaotic attractors in quasiperiodically forced systems exhibit a characteristic signature in their frequency power spectrum that might allow them to be experimentally distinguished from other types of attractors in such systems.

The results of Refs. 7–9 were for specific models, and it is not clear to what extent results (i) and (ii) above apply to the quasiperiodically forced pendulum, Eqs. (1) and (3). It is precisely the aim of the present paper to numerically investigate the existence and properties of strange nonchaotic attractors for the quasiperiodically forced damped pendulum. Specifically, we are primarily interested in the question of typicality (parameter space measure) and in elucidating possible power spectral signatures of these attractors.

By rescaling the independent variable t and letting $\phi = \theta + \pi/2$, Eq. (1) can be written in the form

$$\frac{1}{p} \frac{d^2\phi}{dt^2} + \frac{d\phi}{dt} - \cos\phi = f(t), \quad (4)$$

where p is a new parameter. This is the form of the pendulum equation that we will use in our subsequent work. In the strong damping limit, $p \rightarrow \infty$, Eq. (4) reduces to

$$\frac{d\phi}{dt} - \cos\phi = f(t), \quad (5)$$

which, with $f(t)$ given by Eq. (3), was studied in Refs. 8 and 9 and shown to have strange nonchaotic attractors on a Cantor set of positive measure in the parameters K and V [cf. Eq. (3)].

The analysis of Refs. 8 and 9 makes use of a correspondence of Eqs. (5) and (3) with the Schrödinger equation with quasiperiodic potential. No such analogy exists for Eqs. (4) and (3). Nevertheless, our numerical results strongly suggest that the typicality and spectrum results of Ref. 8 and 9 also hold for Eqs. (4) and (3) for p not too small. This is the main result of this paper. For sufficiently small values of p , Eqs. (4) and (3) exhibit a transition to chaos.

II. CHARACTERIZATION OF THE ATTRACTORS

Before starting with the presentation and discussion of the numerical results we introduce in this section the main quantities used to characterize the attractors, namely, the Lyapunov characteristic exponent, the winding number, the surface of section plot, and the frequency spectrum.

The *Lyapunov characteristic exponent* Λ for an orbit $\phi(t)$ of Eq. (4) is defined by

$$\Lambda = \lim_{T \rightarrow \infty} \left[\frac{1}{T} \ln \left[\frac{d(T)}{d(0)} \right] \right], \quad (6a)$$

where $d(t) = [v^2(t) + \dot{v}^2(t)]^{1/2}$ and $v(t)$ denotes the solution of the linearized equation

$$\frac{1}{p} \frac{d^2v}{dt^2} + \frac{dv}{dt} + v \sin\phi(t) = 0. \quad (6b)$$

Actually, since (6b) is second order, there are two Lyapunov exponents [i.e., two possible results for the limit (6a) depending on the choice of initial conditions for v and \dot{v}]. The largest one is obtained for almost any initial condition and this is the one we calculate and denote Λ hereafter. The other exponent, Λ' , is related to Λ by $\Lambda + \Lambda' + p = 0$ (see Sec. IV).

The *winding number* W for an orbit $\phi(t)$ of Eq. (4) is defined by

$$W = \lim_{T \rightarrow \infty} \left[\frac{\phi(T) - \phi(0)}{T} \right].$$

The *surface of section* plot is obtained by strobing the solution $\phi(t)$ of Eq. (4) at times

$$t_n = \frac{2\pi}{\omega_2} n + t_0,$$

where n is an integer, and plotting

$$\phi_n = \phi(t_n) \pmod{2\pi},$$

versus

$$\theta_n = \omega_1 t_n \pmod{2\pi}.$$

Alternative surface of section plots can be obtained by plotting $\dot{\phi}_n = \dot{\phi}(t_n)$ versus θ_n and ϕ_n versus ϕ_n .

The *frequency spectrum* was obtained by calculating, using a fast Fourier-transform algorithm, the discrete Fourier transform of the sequence $\{s_n\}_{n=0}^{M-1}$ $s_n = h_n p(\phi_n)$, where $p(\phi) = \cos\phi$ and $h_n = \frac{1}{2}[1 - \cos(2\pi n/M)]$; the multiplication by h_n is a smoothing technique corresponding to the so-called method of leakage reduction.^{10,11}

III. NUMERICAL RESULTS

The differential system (4), (3), and (6) was integrated by using a fourth-order Runge-Kutta method with 32 time steps per period of the $\cos\omega_2 t$ driver. The number of driver periods N was taken between 2×10^3 and 2×10^5 , depending on the circumstances. For the fast-Fourier-transform (FFT) algorithm, $M = 2^{16}$ points were used.

In all numerical experiments we have taken $\omega_1 = \frac{1}{2}(\sqrt{5} - 1)$, $\omega_2 = 1$. In most of the experiments the parameter p was fixed at the value $p = 3.0$. The only exceptions are the results of Sec. III E below where this choice of p is discussed and a transition to chaos that occurs for sufficiently small p is illustrated.

A. Lyapunov exponent and winding number

Figure 1 shows a diagram of the K - V plane, giving regions where Λ is negative (hatched) or zero (blank). The

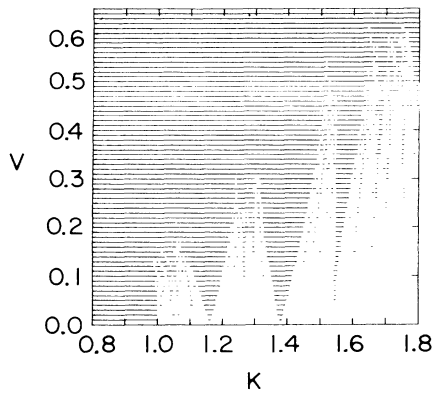


FIG. 1. Diagram of the K - V plane showing regions where $\Lambda < 0$ (hatched) or $\Lambda = 0$ (blank) ($p = 3.0$). The criterion for negative Lyapunov exponent is $\Lambda < -10^{-4}$. A grid of 201 values of K by 66 values of V was used; the integration was taken over a variable number of driver periods going from $N = 2 \times 10^3$ for most cases up to $N = 32 \times 10^3$ for the more slowly converging ones.

criterion for negative Lyapunov exponent used in this figure is $\Lambda < -10^{-4}$. The diagram exhibits a structure similar to the Arnold tongues of the circle map (see, for example, Ref. 12, p. 111).

Figure 2 shows curves of Λ and W as functions of K at a fixed value of V . The curve of W versus K is apparently a “devil’s staircase”: a continuous nondecreasing curve with a dense set of open intervals on which W is constant and given by

$$W = \frac{l}{n}\omega_1 + \frac{m}{n}\omega_2, \quad (7)$$

where l, m, n are integers, and between these intervals there is a Cantor set on which W increases with K . For small K in Fig. 2, Λ is apparently negative on both the Cantor set and the intervals, while for large K , Λ is apparently zero on the Cantor set and negative on the inter-

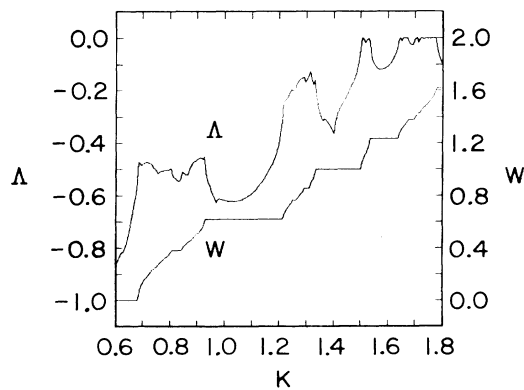


FIG. 2. Curves of the Lyapunov exponent (Λ) and the winding number (W) vs K at $V = 0.55$ ($p = 3.0$, $N = 10^4$).

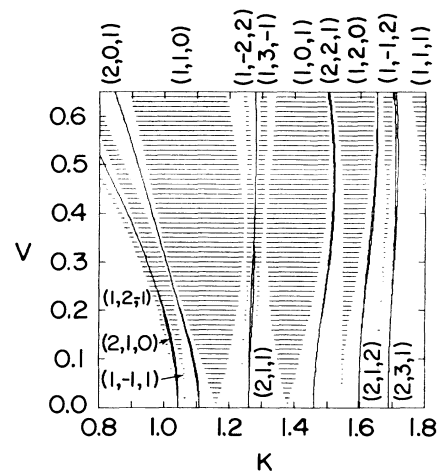


FIG. 3. Diagram of the K - V plane showing the most important resonances identified by the triplet (n, l, m) [cf. Eq. (7)] ($p = 3.0$).

vals. The regions where Eq. (7) holds appear in Fig. 1 as the narrow tongues emerging at small V .

Figure 3 is another diagram of the K - V plane showing the position of the most prominent plateaus of constant winding number identified by the triplets (n, l, m) . It is clear that the $n > 1$ plateaus occupy a very small portion of the parameter space.

In Fig. 4 we have plotted curves giving the K width of several plateaus as a function of V . Note the scale for the $n = 2$ plateau in Fig. 4 has been multiplied by a factor of 5. This plateau is actually the widest of the $n > 1$ plateaus. The figure shows that the width of the plateaus increases from zero to a maximum value, then decrease to practically zero and then increases again [at least from the evidence of the $(1,0,1)$ plateau].

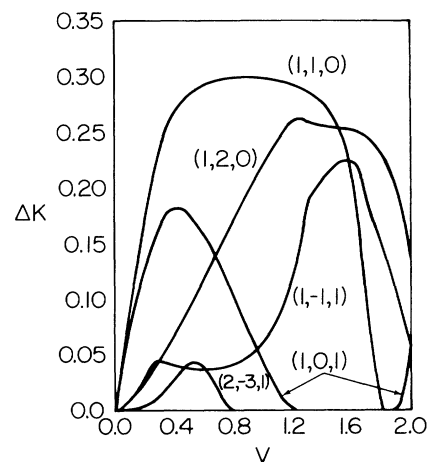


FIG. 4. Curves giving the K width of several resonances as a function of V [note that the width of the $(2,3,1)$ resonance has been multiplied by a factor 5] ($p = 3.0$).

B. Surface of section plots

The three distinct combinations of winding numbers [either satisfying Eq. (7) or not] and Lyapunov exponents (either negative or zero) give rise to surface of section

plots with qualitatively different characteristics—see Table I.

In case *A* the three frequencies W , ω_1 , and ω_2 are incommensurate, and the system will exhibit three-frequency quasiperiodic behavior. A typical orbit gen-

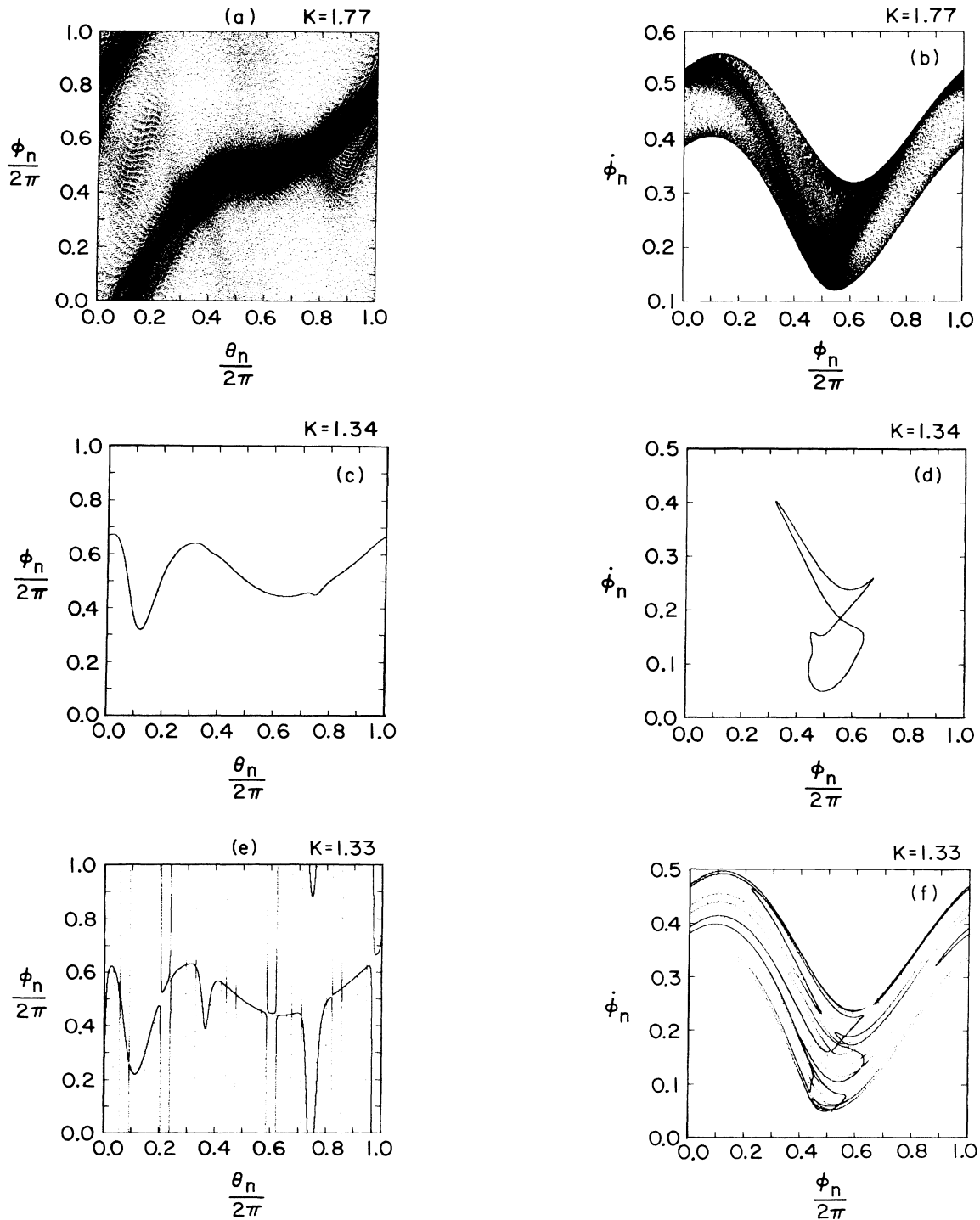


FIG. 5. Surface of section plot of (a),(b) a three-frequency quasiperiodic attractor ($K=1.77$, $V=0.55$, $N=10^5$), (c),(d) a two-frequency quasiperiodic attractor ($K=1.34$, $V=0.55$, $N=10^5$), (e),(f) a strange nonchaotic attractor ($K=1.33$, $V=0.55$, $N=2 \times 10^5$) ($p=3.0$). The corresponding Lyapunov exponents are 0.0, -0.2392 , and -0.0717 , respectively.

TABLE I. Characteristics of attractors.

Case	Winding number	Lyapunov exponent	Type of attractor	Figure
<i>A</i>	$W \neq \frac{l}{n}\omega_1 + \frac{m}{n}\omega_2$	$\Lambda = 0$	Three-frequency quasiperiodic	5(a),5(b)
<i>B</i>	$W = \frac{l}{n}\omega_1 + \frac{m}{n}\omega_2$	$\Lambda < 0$	Two-frequency quasiperiodic	5(c),5(d)
<i>C</i>	$W \neq \frac{l}{n}\omega_1 + \frac{m}{n}\omega_2$	$\Lambda < 0$	Strange nonchaotic	5(e),5(f)

erates a smooth density of points densely filling the surface of section (θ, ϕ) . This is illustrated in Fig. 5(a). In Fig. 5(b) we have also plotted the corresponding surface of section $(\phi, \dot{\phi})$.

In case *B* the frequency W is rationally related to ω_1 and ω_2 and the system will exhibit two-frequency quasiperiodic behavior. The attracting orbit in the surface of section (θ, ϕ) lies on a smooth multivalued curve. If one takes in Eq. (7) l, n and m, n to be relatively prime integers, then n gives the multiplicity of the curve in the surface of section. An example of a two-frequency quasiperiodic attractor is given in Fig. 5(c) (note that in this case $[(n, l, m) = (1, 0, 1)]$, to which corresponds $W = 1$). In Fig. 5(d) we have plotted the corresponding section in the plane $(\phi, \dot{\phi})$.

In case *C* the attractor is geometrically strange: It satisfies a functional relationship $\phi = F(\theta)$ but the function F is discontinuous everywhere. This can be verified in the following way: (i) To verify the existence of the relationship $\phi = F(\theta)$ we initialize a large number of points at a single initial θ value but with different initial $(\phi, \dot{\phi})$ values and find that after a large number N of ω_2 periods, all orbits are attracted to a single pair $(\phi_N, \dot{\phi}_N)$; (ii) that $\phi = F(\theta)$ cannot be a continuous curve follows if the winding number W is irrationally related to ω_1, ω_2 ; (iii) finally, that $\phi = F(\theta)$ is discontinuous everywhere follows from the fact that the map $\theta_{n+1} = \theta_n + 2\pi\omega_1/\omega_2 \pmod{2\pi}$ is ergodic. An example of a strange nonchaotic attractor is given in Figs. 5(e) and 5(f).

We note that according to the Kaplan-Yorke formula

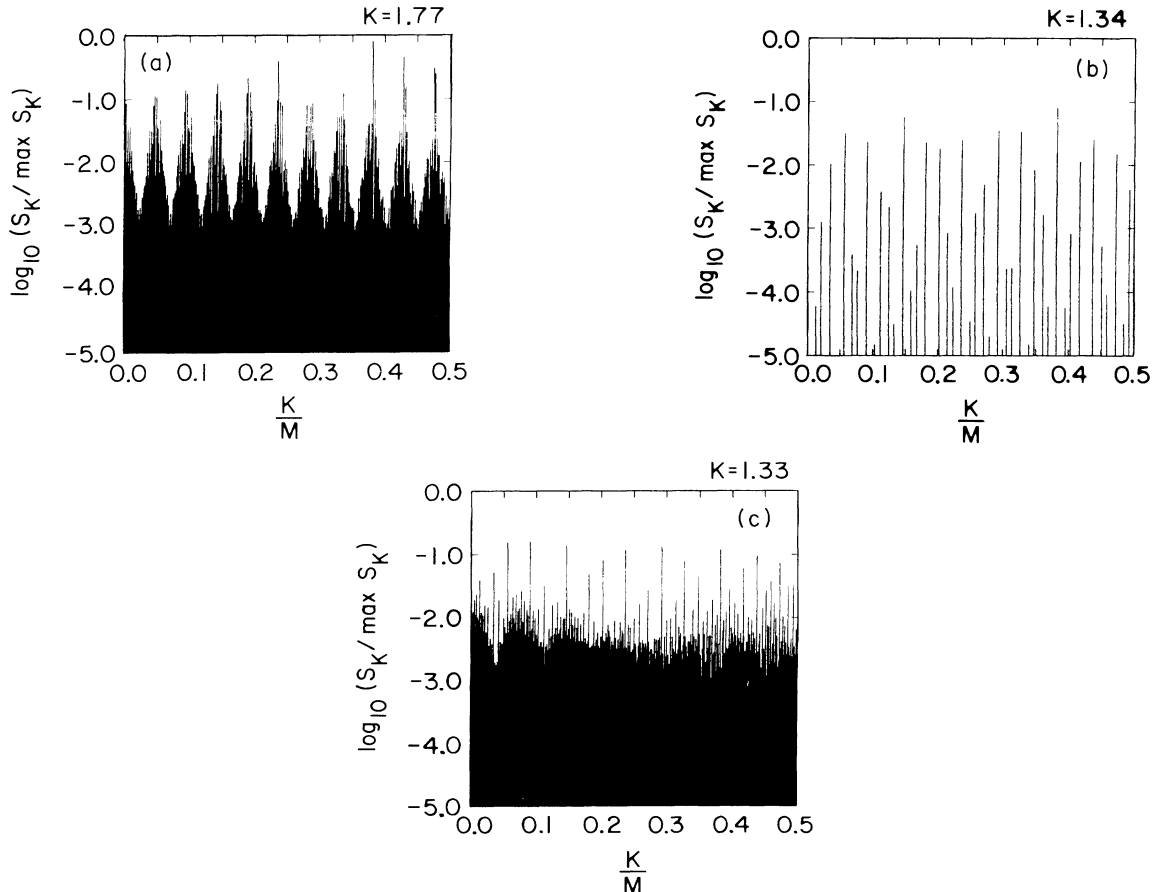


FIG. 6. Frequency spectrum $\{S_k\}_{k=0, M-1}$ of the attractors of (a) Figs. 5(a) and 5(b), (b) Figs. 5(c) and 5(d), (c) Figs. 5(e) and 5(f).

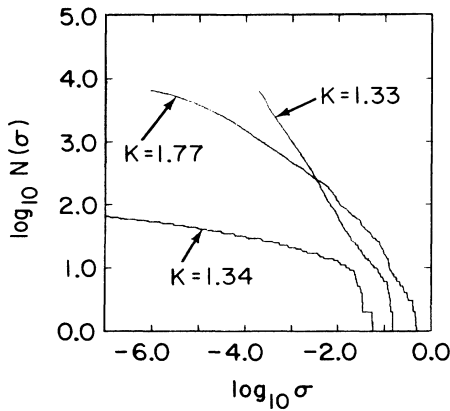


FIG. 7. Spectral distributions of the attractors of Figs. 5(a) and 5(b) ($K=1.77$), Figs. 5(c) and 5(d) ($K=1.34$), Figs. 5(e) and 5(f) ($K=1.33$).

relating Lyapunov numbers to the information dimension^{13,14} the information dimension of these strange nonchaotic attractors is 1 (in the surface of section), since the Lyapunov exponents are zero and negative. We conjecture, however, that the box counting (capacity) dimension¹⁴ is greater than 1 for these attractors.

C. Frequency spectral characteristics

In Figs. 6(a)–6(c) we have plotted the frequency spectra of the orbits which correspond to the surface of section plots of Fig. 5. The figures show the spectrum of the two-frequency quasiperiodic attractor [Fig. 6(b)] is concentrated at a small discrete set of frequencies, while the spectra of both the three-frequency quasiperiodic [Fig. 6(a)] and the strange nonchaotic attractor [Fig. 6(c)] have a much richer harmonic content.

In order to obtain a more quantitative characterization of the spectra of the attractors we introduce a spectral distribution $N(\sigma)$ defined as the number of spectral components larger than some value σ . In Fig. 7 we have plotted the spectral distributions for the three attractors of Fig. 5. It is seen that the strange nonchaotic attractor exhibits distinctive spectral characteristics from the other two. The form of these curves seems to agree with some analytical estimates obtained in Refs. 8 and 9 in the case of Eqs. (5) and (3) and according to which we should have $N(\sigma) \sim \sigma^{-\alpha}$ for strange nonchaotic attractors $N(\sigma) \sim \ln(1/\sigma)$ for two-frequency quasiperiodic attractors, and $N(\sigma) \sim \ln^2(1/\sigma)$ for three-frequency quasiperiodic attractors. The approximately straight line in the log-log plot, Fig. 5, indicating the power-law relationship, $N(\sigma) \sim \sigma^{-\alpha}$, affords an important characteristic signature by means of which strange nonchaotic attractors might be distinguished in experimental situations.

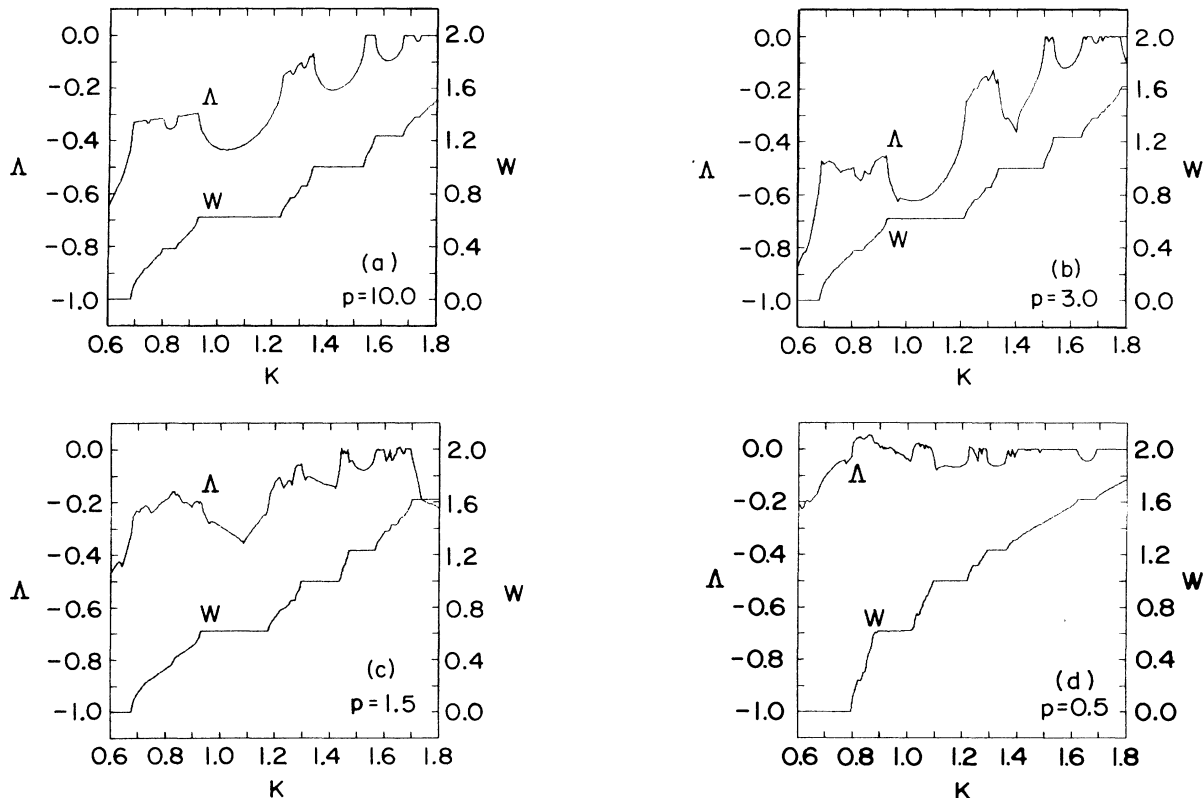


FIG. 8. Curves of Λ and W vs K at $V=0.55$ for the following values of p : (a) 10.0, (b) 3.0, (c) 1.5, and (d) 0.5 ($N=10^4$).

D. Typicality of strange nonchaotic attractors

In the case of Eqs. (5) and (3) a combination of analytical and numerical results indicates that the strange nonchaotic attractors occur on a Cantor set of positive Lebesgue measure in parameter space. Is this measure still positive in the case of Eqs. (4) and (3) or is it zero? In order to try to answer this question we have performed the following numerical experiment. With the parameters p, V fixed at the values of Fig. 2 we have taken the set of K values

$$K^{(i)} = 0.685 + 0.005(i - 1), \quad i = 1, 2, \dots, 49$$

which lie between the widest plateaus $W = 0.0$ and $W = \omega_1$ (the points $K = 0.680$ and 0.930 are already on these plateaus, respectively) and for each of these value we calculated the winding numbers of the orbits with parameters

$$K^{(i)} - \Delta, \quad K^{(i)}, \quad K^{(i)} + \Delta,$$

by integrating Eqs. (4) and (3) over $N = 10^5$ driver periods. When at least two of these three winding numbers are

equal, we say that K is on a plateau, while if they are different, we say that K is on the Cantor set. By proceeding in this way we found that $\frac{41}{49} \approx 84\%$ of points are on the Cantor set. Repeating this study for other small Δ values ($\Delta = 4 \times 10^{-5}, 16 \times 10^{-5}, 64 \times 10^{-5}$), we obtained identical results. These results seem to indicate that the measure of the Cantor set where the strange nonchaotic attractors occur is also positive in the case of the pendulum equation. One observation is in order regarding what we mean by equal and different winding numbers; we found that the distinction between the two cases is always very sharp; for points on the plateaus the difference between the winding numbers is always less than 10^{-8} , while for points on the Cantor set is always larger than 10^{-5} . (This strongly suggests that we are not mistaking many closely spaced narrow plateaus for a Cantor set of positive measure.)

E. Transition to chaos

In order to illustrate how the parameter p affects the behavior of the solutions of Eqs. (4) and (3) we have plot-

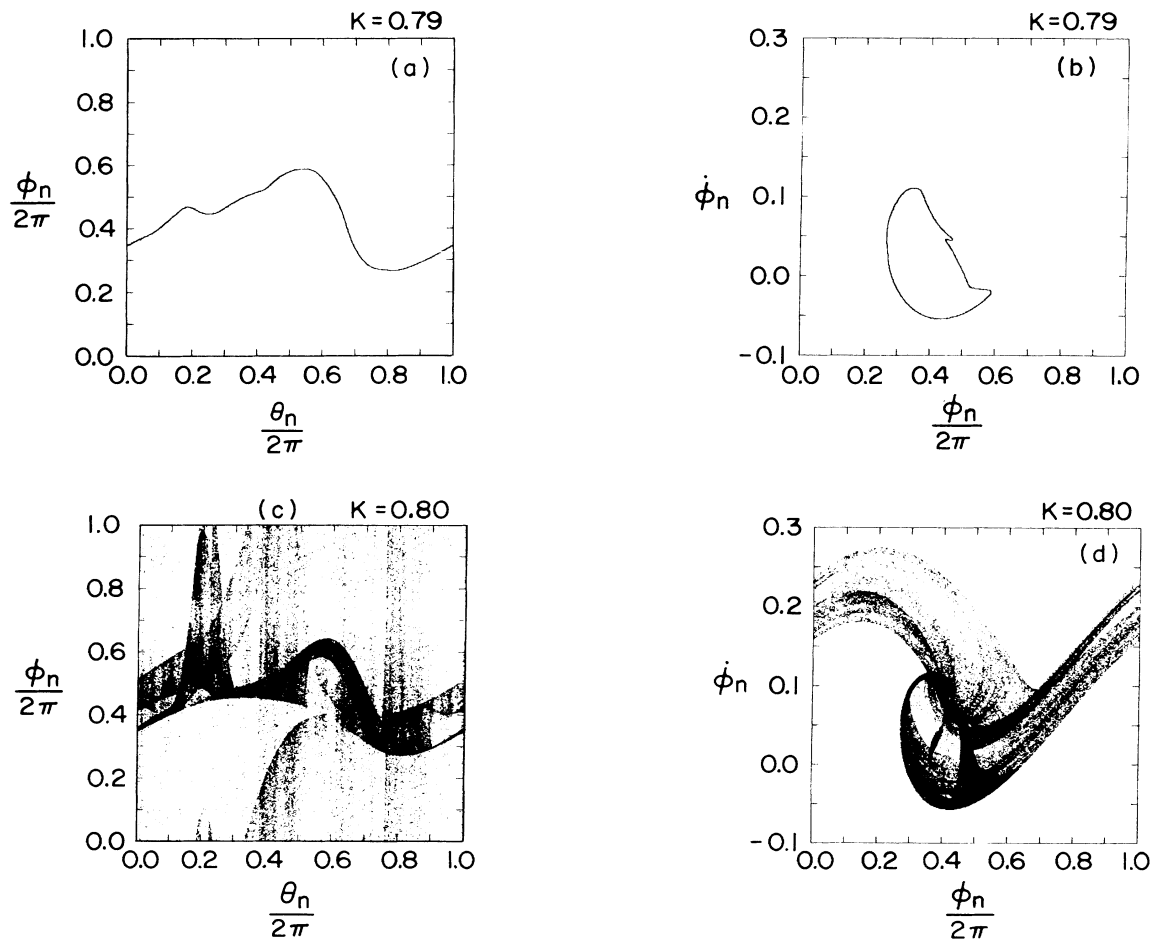


FIG. 9. Surface of section plots of (a),(b) a two-frequency quasiperiodic attractor ($K = 0.79$, $V = 0.55$, $N = 10^5$), (c),(d) a strange chaotic attractor ($K = 0.80$, $V = 0.55$, $N = 2 \times 10^5$) ($p = 0.5$). The corresponding Lyapunov exponents are -0.0359 and $+0.0234$.

ted in Figs. 8(a)–8(d) curves of the Lyapunov exponent (Λ) and the winding number (W) as functions of K , with V fixed, and for several decreasing values of p . Figure 8(a) ($p=10.0$) corresponds to strong damping; as in the limit $p \rightarrow \infty$ Eq. (4) reduces to Eq. (5), it is not surprising that the curves shown in this figure are practically identical to those obtained for Eq. (5) (cf. Fig. 2 in Ref. 9). As the parameter p is decreased the Lyapunov exponent for small K first decreases, reaching a minimum value (for the strange nonchaotic attractors) at approximately $p=3.0$, and then increases again; Fig. 8(b) ($p=3.0$) and Fig. 8(c) ($p=1.5$) show this evolution. For p sufficiently small (less than approximately 1.0), Λ becomes positive, indicating that Eqs. (4) and (3) exhibit chaotic behavior; Fig. 8(d) ($p=0.5$) corresponds to the case where Λ has approximately the largest value. This transition to chaos is illustrated in Fig. 9 where we have plotted the surface of section plots of a two-frequency quasiperiodic attractor [Figs. 9(a) and 9(b)] and a strange chaotic attractor [Figs. 9(c) and 9(d)] for close values of K ($p=0.5$, V fixed). Finally, in the limit $p \rightarrow 0$, Λ becomes zero everywhere.

The above description is mainly about the evolution with p of the Λ versus K curve for small values of K , that is, for values of K for which in the large- p limit strange nonchaotic attractors are present; we have seen that as p decreases below a certain value ($p \simeq 1.0$) these strange nonchaotic attractors disappear in favor of strange chaotic attractors. For large values of K , for which in the large- p limit the system exhibits three-frequency quasiperiodic behavior, the transition to chaos occurs for larger values of p (somewhere between $p=2.5$ and 3.0). This region of positive Lyapunov exponent is barely visible in Fig. 8(c), as the exponent is very small. In the case illustrate in this figure, Eqs. (5) and (3) exhibit both strange nonchaotic and strange chaotic attractors.

IV. COMPARISON WITH PREVIOUS RESULTS

Our stroboscopic sampling of Eqs. (4) and (3) at the times $t = t_n = 2\pi n / \omega_2 + t_0$ defines a three-dimensional invertible map,

$$(\phi_{n+1}, \dot{\phi}_{n+1}) = G(\phi_n, \dot{\phi}_n, \theta_n), \quad (8a)$$

$$\theta_{n+1} = (\theta_n + 2\pi / \omega_2) \pmod{2\pi}. \quad (8b)$$

Formally setting $p = \infty$, Eq. (4) becomes Eq. (5), and the corresponding invertible map is two dimensional,

$$\phi_{n+1} = g(\phi_n, \theta_n) \pmod{2\pi}, \quad (9a)$$

$$\theta_{n+1} = (\theta_n + 2\pi / \omega_2) \pmod{2\pi}. \quad (9b)$$

Thus Eqs. (9) define an invertible map on a two torus. Our results of Ref. 9 showed that for the class of functions g resulting from surface of sections of $d\phi/dt = \bar{g}(\phi, t)$ where the t dependence of \bar{g} is quasiperiodic, Eqs. (9) typically (in the sense discussed previously) had strange nonchaotic attractors. When we make p finite, we add an additional phase space dimension, namely, $\dot{\phi}$. Our numerical results here show that for sufficiently large p , the addition of the new dimension does not qualitatively change the situation. That is, the results are the same as would be expected for a map on a two torus with the form of Eqs. (9). Thus, although the phase

space is four dimensional ($\phi, \dot{\phi}, \theta = \omega_1 t, \xi = \omega_2 t$), it is apparently the case that there is an embedded three torus to which all orbits are attracted, and on which (with some suitable change of the ϕ coordinate) the dynamics is described by an equation of the form $d\phi/dt = \bar{g}(\phi, t)$. It is on this torus that the quasiperiodic and strange nonchaotic attractors of Figs. 5 lie. No chaos with positive Lyapunov exponent is possible as long as this situation applies [it is ruled out for Eqs. (9) with invertible g]. Our transition to chaos (Sec. III E) means that the solutions are no longer attracted to a smooth toroidal surface. Presumably, what happens is that, as p is reduced, the toroidal surface “fractures” in a way somewhat analogous to what happens for two-dimensional circle maps at criticality. (This, however, has not been investigated here.) The main point is that the introduction of *finite* large p does not immediately destroy the existence and typicality of strange nonchaotic attractors. (In this respect the limit $p \rightarrow \infty$ is nonsingular.) In fact, the critical value of p found in Sec. III E was fairly small, $p_c \simeq 1$.

In order to see why the torus might be preserved with finite p we recall from Sec. II that there were two Lyapunov exponents, Λ and Λ' (we take $\Lambda \geq \Lambda'$) which satisfy

$$\Lambda' = -(\Lambda + p). \quad (10)$$

For $p > p_c$ both Λ and Λ' are negative. Equation (10) follows if we view (4) as defining a time dependent [because of $f(t)$] flow in $(\phi, \dot{\phi})$ space, $d\dot{\phi}/dt = -p(\dot{\phi} - \cos\phi) + f(t)$, $d\phi/dt = \dot{\phi}$. Taking the divergence of this flow, we obtain

$$\frac{\partial}{\partial \dot{\phi}} \left[\frac{d\dot{\phi}}{dt} \right] + \frac{\partial}{\partial \phi} \left[\frac{d\phi}{dt} \right] = -p.$$

Equation (10) results, since this divergence is also the sum of the Lyapunov exponents [$-(\Lambda + \Lambda')$ is the exponential rate at which areas in $(\phi, \dot{\phi})$ space, contract]. For large p we expect and numerically find Λ to be close to its value for the $p = \infty$ case [Eq. (5)]. Thus from (10), large p implies that Λ' is a large negative number. We may view $-\Lambda'$ as the exponential rate at which orbits in the three-dimensional $(\phi, \dot{\phi}, \theta)$ phase space of Eqs. (8) are attracted to the torus. For large p this rate is very rapid, and thus the torus would be expected to be rather stable and difficult to destroy. As p decreases $-\Lambda'$ becomes smaller; eventually, at $p = p_c$, the nonlinearity overpowers the contraction to the torus and destroys it.

Arguments similar to these lead us to believe that strange nonchaotic attractors should be common and occur typically for general two-frequency quasiperiodically forced nonlinear systems of arbitrarily high dimensionality. Basically, what we require is that orbits be attracted to a two torus on which the dynamics are described by Eqs. (9). Clearly this can happen for systems of greater dimensionality than Eqs. (3) and (4) (including infinite dimensional systems).

V. CONCLUSIONS

We have discussed the existence and properties of strange nonchaotic attractors exhibited by the damped

pendulum equation with two-frequency quasiperiodic forcing, Eqs. (4) and (3).

In particular, the pendulum equation apparently exhibits strange nonchaotic attractors and these attractors are typical in the sense that they exist on a set (a Cantor set) of positive Lebesgue measure in parameter space. Besides these attractors the equation exhibits two- and three-frequency quasiperiodic behavior, respectively, on a dense set of intervals and on a Cantor set in parameter space.

In addition, the strange nonchaotic attractors apparently have distinctive spectral characteristics which may make them observable in experiments involving physical nonlinear phenomena which can be modeled by the damped forced pendulum equation (e.g., Josephson junc-

tions and sliding charge-density waves). We have also verified, but not studied in any detail, that for sufficiently small damping, the equation exhibits a transition to chaos.

ACKNOWLEDGMENTS

This work was supported by the U.S. Department of Energy [Office of Basic Energy Sciences (Applied Mathematics Program)] and by the U.S. Office of Naval Research. One of us (F.R.) was also supported by the Portuguese Instituto Nacional de Investigação Científica during his sabbatical leave from the Instituto Superior Técnico of the Universidade Técnica de Lisboa.

*Permanent address: Centro de Electrodinâmica da Universidade Técnica de Lisboa, Instituto Superior Técnico, 1096 Lisboa Codex, Portugal.

¹A. Aiello, A. Barone, and G. A. Ovsyannikov, *Phys. Rev. B* **30**, 456 (1984); P. Alstrom, M. H. Jensen, and M. T. Levinsen, *Phys. Lett.* **103A**, 171 (1984); P. Alstrom and M. T. Levinsen, *Phys. Rev. B* **31**, 2753 (1985); P. Bak, T. Bohr, M. H. Jensen, and P. V. Christiansen, *Solid State Commun.* **51**, 231 (1984); M. R. Beasley, and B. A. Huberman, *Comments Solid State Phys.* **10**, 155 (1982); V. N. Belykh, N. F. Pedersen, and O. H. Soerensen, *Phys. Rev. B* **16**, 4853 (1977); **16**, 4860 (1977); E. Ben-Jacob and D. J. Bergman, *Phys. Rev. A* **29**, 2021 (1984); E. Ben-Jacob, Y. Braiman, R. Shainsky, and Y. Imry, *Appl. Phys. Lett.* **38**, 822 (1984); E. Ben-Jacob, I. Goldhirsch, Y. Imry, and S. Fishman, *Phys. Rev. Lett.* **49**, 1599 (1982); T. Bohr, P. Bak, and M. H. Jensen, *Phys. Rev. A* **30**, 1970 (1984); Y. Braiman, E. Ben-Jacob, and Y. Imry, *IEEE Trans. Magn.* **MAG-17**, 784 (1981); M. Cirillo and N. F. Pedersen, *Phys. Lett.* **90A**, 150 (1982); D. C. Cronemeyer, C. C. Chi, A. Davidson, and N. F. Pedersen, *Phys. Rev. B* **31**, 2667 (1985); Z. D. Genchev, Z. G. Ivanov, and B. N. Todorov, *IEEE Trans. Circuits Syst.* **CAS-30**, 633 (1983); I. Goldhirsch, Y. Imry, G. Wasserman, and E. Ben-Jacob, *Phys. Rev. B* **29**, 1218 (1984); V. N. Gubankov, K. I. Konstantinyan, V. P. Koshelets, and G. A. Ovsyannikov, *Pis'ma Zh. Tekhn. Fiz.* **8**, 1332 (1982) [*Sov. Tech. Phys. Lett.* **8**, 574 (1982)]; *IEEE Trans. Mag.* **MAG-19**, 637 (1983); V. N. Gubankov, S. L. Ziglin, K. I. Konstantinyan, V. P. Koshelets, and G. A. Ovsyannikov, *Zh. Eksp. Teor. Fiz.* **86**, 343 (1984) [*Sov. Phys.—JETP* **59**, 198 (1984)]; E. G. Gwinn and R. M. Westervelt, *Phys. Rev. Lett.* **54**, 1613 (1985); *Phys. Rev. A* **33**, 4143 (1986); D.-R. He, W. J. Yeh, and Y. H. Kao, *Phys. Rev. B* **30**, 172 (1984); **31**, 1359 (1985); Q. Hu, J. U. Free, M. Iansiti, O. Liengme, and M. Tinkham, *IEEE Trans. Magn.* **MAG-21**, 590 (1985); B. A. Huberman, J. P. Crutchfield, and N. H. Packard, *Appl. Phys. Lett.* **37**, 750 (1980); D. D'Humieres, M. R. Beasley, B. A. Huberman, and A. Libchaber, *Phys. Rev. A* **26**, 3483 (1982); M. Iansiti, Q. Hu, R. M. Westervelt, and M. Tinkham, *Phys. Rev. Lett.* **55**, 746 (1985); M. Inoue and H. Koga, *Prog. Theor. Phys.* **68**, 2184 (1982); M. J. Kajanto and M. M. Salomaa, *Solid State Commun.* **53**, 99 (1985); R. L. Kautz, *J. Appl. Phys.* **52**, 3528 (1981); **52**, 6241 (1981); *IEEE Trans. Magn.* **MAG-19**, 465 (1983); *J. Appl. Phys.* **58**, 424 (1985); R. L. Kautz and J. C. Macfarlane, *Phys. Rev. A* **33**, 498 (1986); R. L. Kautz and R.

Monaco, *J. Appl. Phys.* **57**, 875 (1985); H. Koga, H. Fujusaka, and M. Inoue, *Phys. Rev. A* **28**, 2370; Z. J. Kowalik, *Acta Phys. Pol. A* **64**, 357 (1983); M. Levi, F. C. Hoppensteadt, and W. L. Miranker, *Q. Appl. Math.* **36**, 167 (1978); M. T. Levinsen, *J. Appl. Phys.* **53**, 4294 (1982); A. H. MacDonald and M. Plischke, *Phys. Rev. B* **27**, 201 (1983); P. M. Marcus, Y. Imry, and E. Ben-Jacob, *Solid State Commun.* **41**, 161 (1982); R. F. Miracky and J. Clarke, *Appl. Phys. Lett.* **43**, 508 (1983); D. E. McCumber, *J. Appl. Phys.* **39**, 3113 (1968); R. F. Miracky, J. Clarke, and R. H. Koch, *Phys. Rev. Lett.* **50**, 856 (1983); R. F. Miracky, M. H. Devoret, and J. Clarke, *Phys. Rev. A* **31**, 2509 (1985); M. Octavio, *Phys. Rev. B* **29**, 1231 (1984); M. Octavio and C. R. Nasser, *ibid.* **30**, 1586 (1984); M. Odyniec and L. O. Chua, *IEEE Trans. Circuits Syst.* **CAS-30**, 308 (1983); **CAS-32**, 34 (1985); K. Okuyama, H. J. Hartfuss, and K. H. Gundlach, *J. Low Temp. Phys.* **44**, 283 (1981); N. F. Pedersen and A. Davidson, *Appl. Phys. Lett.* **39**, 830 (1981); N. F. Pedersen, M. R. Samuelsen, and K. Saermark, *J. Appl. Phys.* **44**, 5120 (1973); N. F. Pedersen, O. H. Soerensen, B. Duelholm, and J. Mygind, *J. Low Temp. Phys.* **38**, 1 (1980); K. Sakai and Y. Yamaguchi, *Phys. Rev. B* **30**, 1219 (1984); F. M. A. Salam and S. S. Sastry, *IEEE Trans. Circuits Syst.* **CAS-32**, 784 (1985); H. Seifert, *Phys. Lett.* **98A**, 213 (1983); **101A**, 230 (1984); W.-H. Steeb and A. Kunick, *Phys. Rev. A* **25**, 2889 (1982); W. C. Stewart, *Appl. Phys. Lett.* **12**, 277 (1968); C. Vanneste *et al.*, *Phys. Rev. B* **31**, 4230 (1985); W. J. Yeh, D.-R. He, and Y. H. Kao, *Phys. Rev. Lett.* **52**, 480 (1984); W. J. Yeh and Y. H. Kao, *ibid.* **49**, 1888 (1982); W. J. Yeh and Y. H. Kao, *Appl. Phys. Lett.* **42**, 299 (1983).

²T. Bohr, P. Bak, and M. H. Jensen, *Phys. Rev. A* **30**, 1970 (1984); S. E. Brown, G. Mozurkewich, and G. Gruner, *Phys. Rev. Lett.* **52**, 2277 (1984); G. Gruner, *Phys. Scr.* **32**, 11 (1985); G. Gruner, A. Zawadowski, and P. M. Chaikin, *Phys. Rev. Lett.* **46**, 511 (1981); A. H. MacDonald and M. Plischke, *Phys. Rev. B* **27**, 201 (1983); A. Zettle and G. Gruner, *Solid State Commun.* **46**, 501 (1983); *Phys. Rev. B* **29**, 755 (1984).

³D.-R. He, W. J. Yeh, and Y. H. Kao, *Phys. Rev. B* **30**, 172 (1984).

⁴G. A. Held and C. Jeffries, *Phys. Rev. Lett.* **56**, 1183 (1986).

⁵J. P. Sethna and E. D. Siggia, *Physica* **11D**, 193 (1984).

⁶K. Kaneko, *Prog. Theor. Phys.* **71**, 282 (1984).

⁷C. Grebogi, E. Ott, S. Pelikan, and J. A. Yorke, *Physica* **13D**, 261 (1984).

⁸A. Bondeson, E. Ott, and T. M. Antonsen, *Phys. Rev. Lett.* **55**, 2103 (1985).

- ⁹F. J. Romeiras, A. Bondeson, E. Ott, T. M. Antonsen, and C. Grebogi, *Physica D* (to be published).
- ¹⁰E. O. Brigham, *The Fast Fourier Transform* (Prentice-Hall, Englewood Cliffs, N.J., 1974).
- ¹¹G. E. Powell and I. C. Percival, *J. Phys. A* **12**, 2053 (1979).
- ¹²R. L. Devaney, *An Introduction to Chaotic Dynamical Systems* (Benjamin/Cummings, Menlo Park, CA., 1986).
- ¹³J. Kaplan and J. A. Yorke, *Functional Differential Equations and the Approximation of Fixed Points* (Springer, Berlin, 1978), p. 228.
- ¹⁴J. D. Farmer, E. Ott, and J. A. Yorke, *Physica* **7D**, 153 (1983).